



## BEAMFORMING ON A TURBOFAN ENGINE IN AN INDOOR TEST-FACILITY

H.A. Siller<sup>1</sup>, S. Schröder<sup>1</sup>,  
G. Saueressig<sup>2</sup>, S. Fröhlich<sup>3</sup>

<sup>1</sup>DLR, German Aerospace Center

Institute of Propulsion Technology, Engine Acoustics,  
Berlin, Germany;

<sup>2</sup>Deutsche Lufthansa AG Umweltkonzepte Konzern,  
Frankfurt, Germany;

<sup>3</sup>Lufthansa Technik AG, System Engineering Services, HAM WT31,  
Hamburg, Germany.

February 19, 2008

### ABSTRACT

This paper describes the progress of an ongoing project with the ultimate goal to develop a method for acoustic indoor tests of aircraft engines. Measurements with a turbofan aircraft engine in the indoor test-stand of Lufthansa Technik are described. A linear microphone array has been set up using a special arrangement that has been patented by DLR that minimises the effect of reflected sound waves. It is demonstrated that with a beamforming algorithm that uses a small, 'sliding' sub-array, it is possible to measure differences between the sound fields of different engine modifications.

## 1 INTRODUCTION

Aircraft noise has become a limiting factor for the growth of air traffic. Noise limits for aircraft become increasingly stringent and individual airports in densely populated urban regions impose their own limits or restriction, mainly on nighttime operations. Because of the long time an aircraft remains in service, aircraft operators cannot wait for the next generations of aircraft with lower

noise emissions, but have to look whether there are any noise abatement measures that can be retro-fitted to their fleet in service. For these reasons, Lufthansa AG and Lufthansa Technik have been cooperating with DLR successfully over the last seven years in several noise related research projects.

Aircraft engine noise can be measured in flight using phased arrays [12], [5], or [9], but these tests are very expensive. In order to diagnose special problems of engine noise, a combination of fly-over array measurements with static engine tests can be useful. This approach has been taken for an investigation of noise emissions of the MD-11 aircraft during landing approach, where data from flyovers with a Lufthansa cargo MD-11 were analysed in combination with static measurements from the indoor test stand of Lufthansa Technik in Hamburg [7].

Static tests of aircraft engines are performed during certification on special open-air test sites. These measurements are still very expensive because of their limited availability, weather and community noise restrictions.

It would therefore be helpful, if acoustic test could be performed indoors in the same test-facilities, where the engines are regularly tested for performance out after their final assembly or after a repair job or service check.

In the German national research programme LEXMOS, DLR and Rolls-Royce Deutschland have started to develop an indoor technique for engine noise test which has been described in Böning et al. [2] and has also been presented at the first BeBeC in 2006 [3]. The experience gained so far has led to the development of the microphone arrangement that was used for the experiments used here, where Lufthansa Technik, Lufthansa AG, and DLR cooperated in an experiment with a large turbofan engine.

The test was performed at the indoor engine test facility of Lufthansa Technik in Hamburg. DLR set up their patented linear microphone array, which runs parallel with the engine axis along the inner edge of the room between the side wall and the floor. This set-up keeps the microphones from receiving sound waves which have been reflected from the side wall and the floor. This idea was developed on the basis of the experience DLR had with linear microphone arrays at open air engine tests [11], [1] and the works of Guidati et al. [6] and Sijtsma and Holthusen [10] on the problems of beamforming in reverberating environments.

## 1.1 Experimental set-up

Figure 1 shows a schematic of the test-section with the engine. The engine is suspended from the roof and is equipped with a hard-wall bell-mouth inlet (see figure 2). This type of inlet is typically used for indoor tests because it ensures an even inflow into the engine.

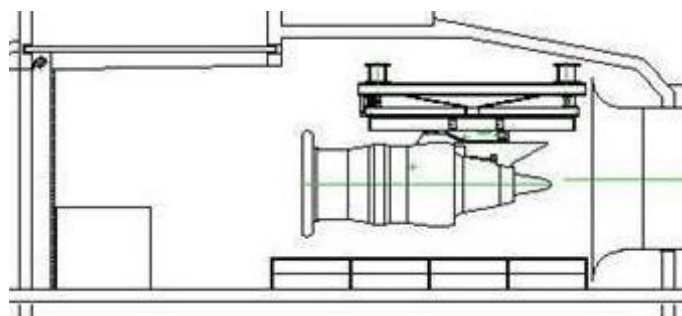


Figure 1: The test-cell of LHT in Hamburg

The microphone array was set up along the right-hand side wall when looking upstream (see figure 3). Figure 4 shows how the microphones were mounted on a wooden assembly with an L-shaped profile. This gave a hard-wall acoustic boundary condition and ensured mechanical stability for the microphones and the cabling. The data acquisition unit was placed downstream of the engine and all movable parts had been tightly secured in order to avoid any parts being ingested by the engine.



Figure 2: The engine with the bell-mouth inlet in the test-cell



Figure 3: Linear microphone array along the side-wall of the test-cell

The microphone array was 6.6 m long and consisted of 56 microphones that were arranged with a constant distance of 0.12 m. It extended from 6.12 m upstream of the engine inlet to -0.5 m downstream, covering a range of the emission angle between  $38^\circ < \theta < 96^\circ$ .

The data acquisition system with 128 channels consisted of two parts, the main computer with the user interface and the data storage and the analogue-to-digital conversion unit that was located in the test-cell. The main computer was placed in the control room.

The data were acquired with a sampling frequency of  $f_s = 32768$  Hz for  $t_s = 24.98$  s at each static test point. In addition to the 56 microphone signals, a signal for the shaft speed of the



*Figure 4: Linear microphone array along the side-wall of the test-cell*

primary shaft was recorded. This signal could later be used to determine the shaft speed and track the stability of the engine speed.

The microphones were calibrated by recording one second of data for each microphone with a pistonphone as a reference noise source.

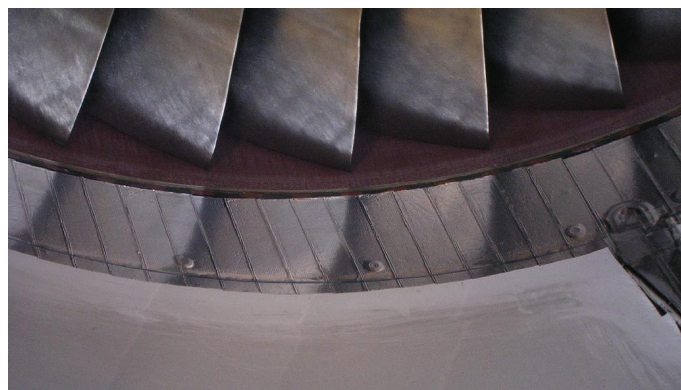


*Figure 5: The casing liner covered with high-speed tape*

## 1.2 Experimental results

Experiments were performed with two different configurations of the engine: for build 1, the casing liner of the engine completely covered with high-speed tape (see figure 5). This modification

gave a hard-wall boundary condition at the fan casing. For build 2, the standard configuration with the liner was restored by removing the tape from the casing liner.

The data were processed by first calibrating the individual microphone tracks using the calibration data tracks. Then, the cross-spectral matrices were calculated for every test run. The FFTs were run with Hanning windows of 1024 samples with an overlap of 50%. A higher frequency resolution would have been possible, but was not used because the engine tones are well separated.

The shaft speed was calculated from the the shaft speed signal data. Narrow band spectra were converted to engine order (EO) spectra by scaling the frequency axis with the engine shaft speed.

The cross spectral matrices were used as input for the beamforming algorithm in the frequency domain. A moving sub-array of 11 microphones was focused on the engine inlet region. By moving the sub-array along the linear array, advancing by one microphone at each step, the directivity of the engine inlet was investigated. The moving sub-array covered a range of  $41^\circ < \theta < 89^\circ$  of the emission angle relative to the engine inlet.

Figure 6 presents the results for build 1 (hard-wall fan casing) with an engine speed of  $N1 = 78\%$ , which is about 20% above a typical speed during landing approach.

In figure 6, the vertical frequency axis is scaled in engine orders. The horizontal axis shows the emission angle  $\theta$  relative to the centre microphone of each sub-array. Horizontal lines are engine tones, the most prominent ones occur at multiples of the blade passing frequency (BPF). The fan has 38 blades, so the BPF harmonics show up at engine orders 38 (BPF), 76 (2 BPF), 114 (3 BPF), 152 (4 BPF), and so on.

Additionally, there are interaction tones between the fan and the first booster stage, which has 62 blades. According to the extension of the theory of Tyler and Sofrin [13] to multiple rotors and stators [4], [8]), the tones at engine orders 100 and 138 can be explained as interaction tones between the 38 fan blades and the 62 blades of the first booster stage.

The frequencies of the interaction tones are

$$f = h_1 B_1 s_1 - h_2 B_2 s_2,$$

where  $h$  are arbitrary integers,  $B$  the blade counts and  $s$  the shaft frequencies. Because both stages operate on the same shaft, they have the same frequency  $s = s_1 = s_2$  and the engine order of the interaction tone is

$$EO = \frac{f}{s} = h_1 B_1 - h_2 B_2.$$

With  $B_1 = 38$  and  $B_2 = 62$ , we get  $EO = 100$  with  $h_1 = 1$  and  $h_2 = -1$  and  $EO = 138$  with  $h_1 = 2$  and  $h_2 = -1$ .

Figure 12 presents the results for build 2, with the standard casing liner.

In figure 8, the sound pressure levels of figure 6 have been subtracted from 7. Negative values, shown in blue, indicate a decrease of the sound pressure levels when the casing liner is active, while positive values, shown in red, stand for increased levels.

Surprisingly, the casing liner increases the sound pressure levels of the BPF tone and its harmonics. This increase is very strong with levels up to 9.6 dB while the decrease in broad-band noise between the BPF tones is relatively moderate with about  $-2$  dB. This increase in the BPF tones is most likely caused by mode scattering at the liner splices. The liner is built from six segments with hard-wall splices that interrupt the lined surfaces. These splices form a discontinuity for the rotating sound field that is generated by the fan. Energy is being transferred into modes that are able to propagate and the sound pressure levels at BPF and its harmonics increase.

The point spread functions for several engine tones are presented in figure 9 for an emission angle of  $\theta = 81^\circ$  and in figure 10 for  $\theta = 46^\circ$ . The figures show the sound pressure level calculated for the given sub-array with the focus moving along the engine axis.

For a sub-array near the engine inlet, at  $\theta = 81^\circ$ , the peaks for the sources are well visible and the beam widths are relatively narrow. The peaks, however, occur not at the front face of the engine inlet, but about 0.4 m inside the engine. This is due to a refraction of the sound waves at the mouth of the inlet barrel.

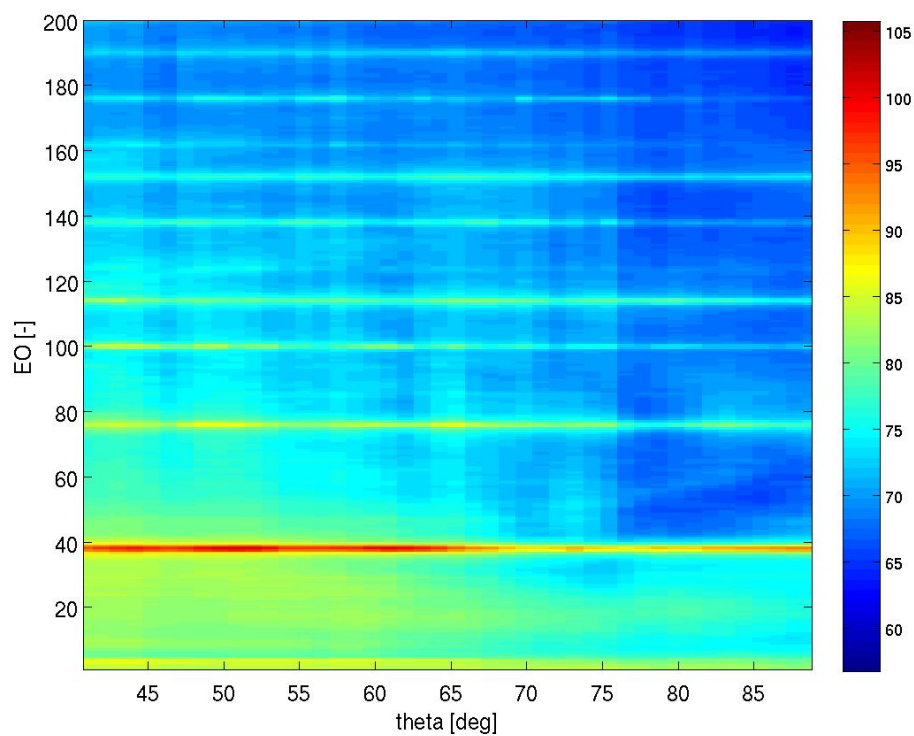


Figure 6: Moving sub-arrays of 11 microphones focused on the engine inlet, build 1 with covered inlet liner, shaft speed 78% NI

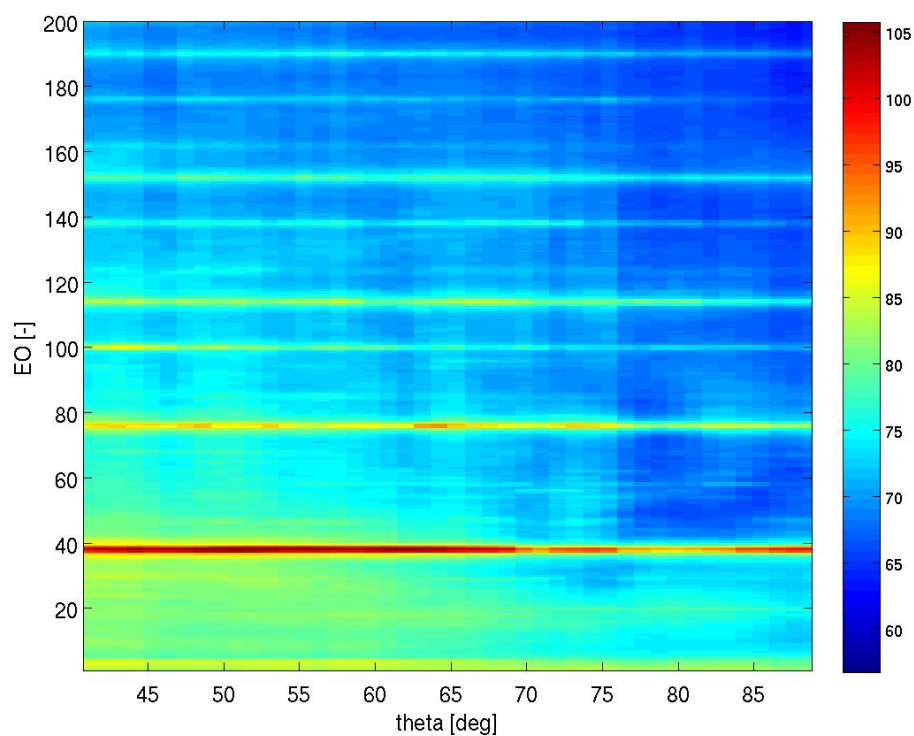


Figure 7: Moving sub-arrays of 11 microphones focused on the engine inlet, build 2 with lined inlet, shaft speed 78% NI

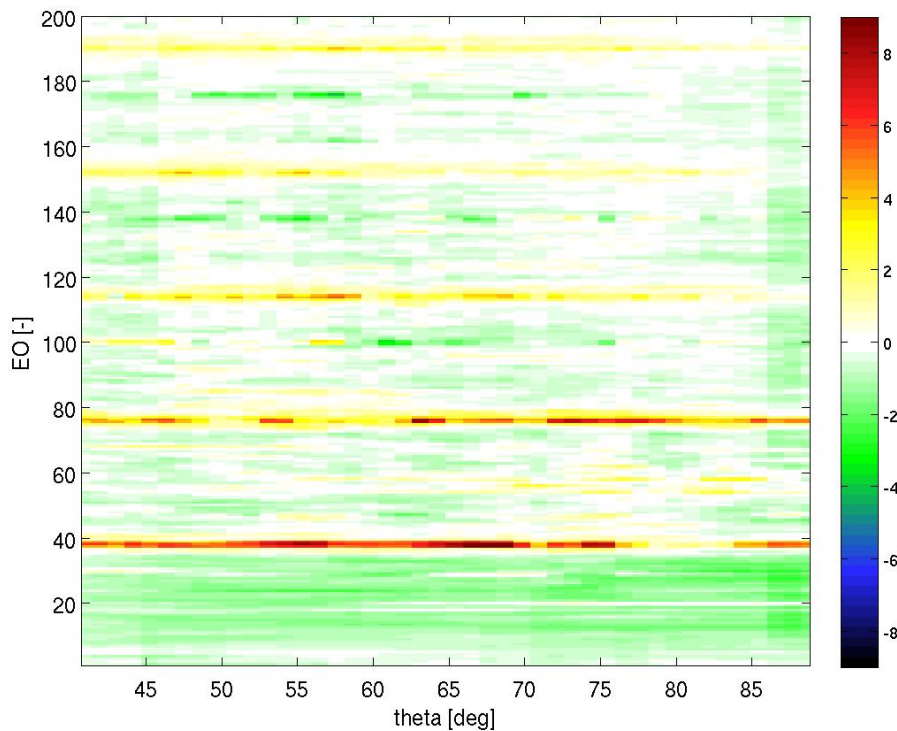


Figure 8: Moving sub-arrays of 11 microphones focused on the engine inlet, difference between build 2 (hard wall fan casing) and build 1 (lined fan casing), shaft speed 78% NI

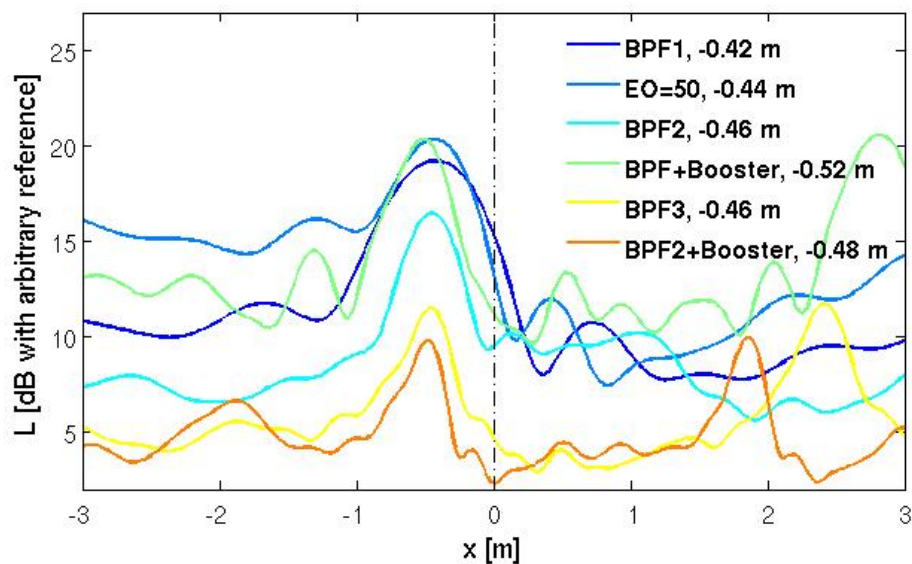


Figure 9: Point spread functions for different engine tones for  $\theta = 46^\circ$ , shaft speed 78% NI

For the sub-array at  $\theta = 46^\circ$ , the effective size of the array is reduced by the projection of the array onto the plane perpendicular to the ray from the centre microphone of the array and the focus point on the engine axis. The reduced array size results in a larger beamwidth, because the beamwidth

$$B \sim \frac{\lambda r}{l}$$

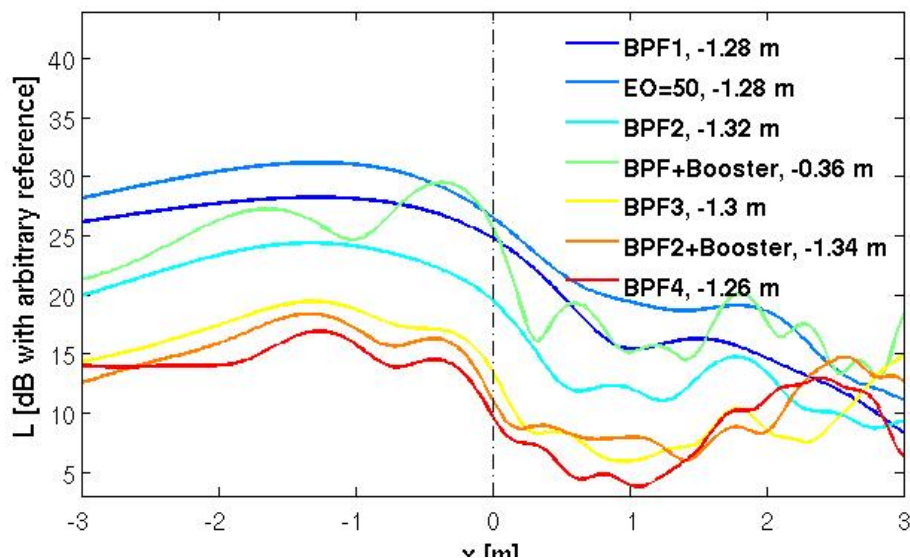


Figure 10: Point spread functions for different engine tones for  $\theta = 46^\circ$ , shaft speed 78% NI

is directly proportional to the wavelength  $\lambda$  and the distance from the array to the focus  $r$  and inversely proportional to the effective length of the array  $l$ , i.e. the projection of the array in the direction of the focus.

Figures 9 and 10 also show, that the focus is not at the same position for every frequency line. When the shift in the source position is taken into account by first searching the maximum along the engine axis and then plotting the sound pressure level at this position, the distribution of sound pressure levels as a function of emission angle and frequency is different from that for the fixed focus.

Figures 11 for build 1 and 12 for build 2 illustrate this effect. The sound pressure levels are generally higher, because the focus is now at the maximum position of the point spread function.

Also, an additional tone at  $EO = 50$  occurs at small emission angles that was not visible when the focus was at the front face of the engine inlet.

## 2 CONCLUSIONS

Measurements on a turbofan engine in an indoor test-facility with a linear microphone array have been presented. Sub-arrays with a constant number of microphones have been focused on the engine inlet from different emission angles. The sound pressure levels from the focused narrow band spectra have been presented as a function of the emission angle and of the frequency scaled in engine orders.

The effective array size is reduced when sub-arrays at small emission angles are used. The beamwidth of these arrays is increased. The closer the sub-array is chosen towards an emission angle of  $\theta = 90^\circ$ , the smaller the beamwidth.

When the sound sources are searched by moving the focus of a given sub-array along the axis of the engine, the sources are found inside the engine because of the refraction of the sound waves at the engine inlet.

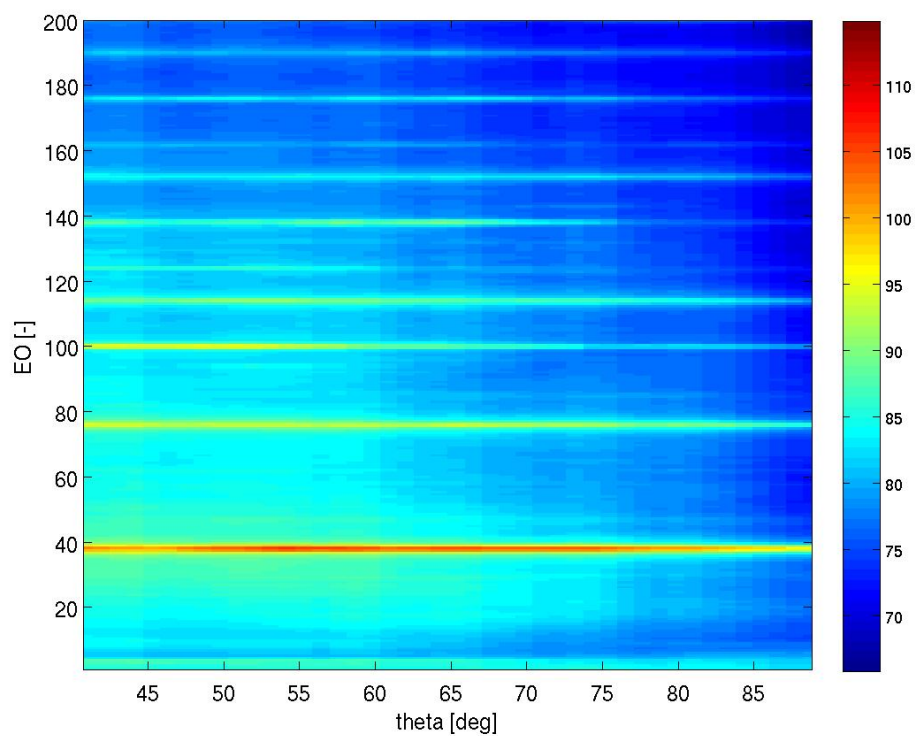


Figure 11: Moving sub-arrays of 11 microphones with maximum search along the engine axis near the inlet, build 1 with covered inlet liner, shaft speed 78% N1  
n the

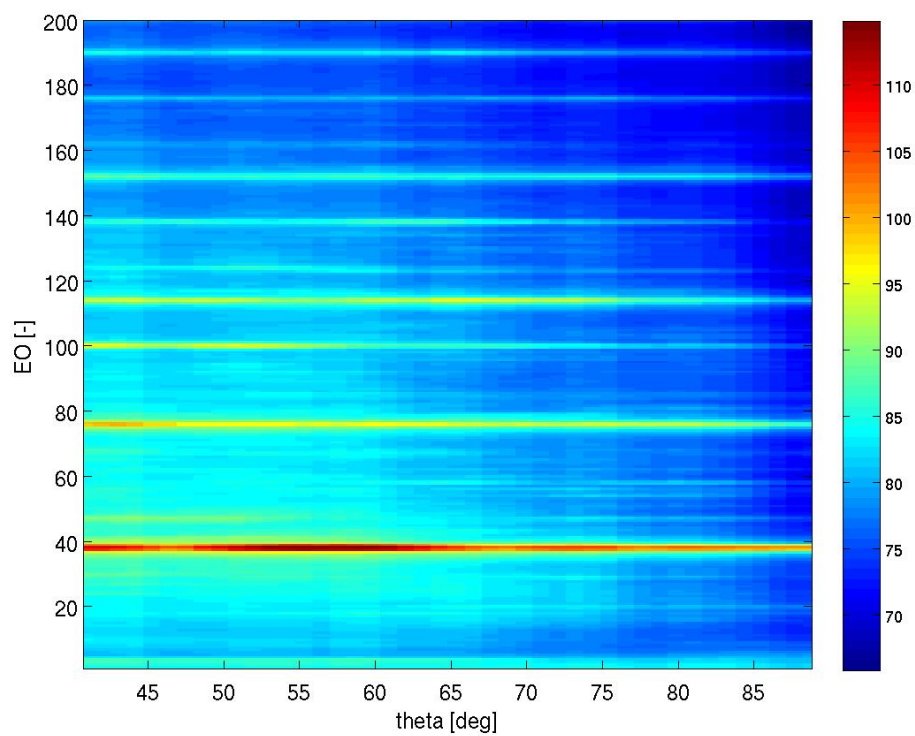


Figure 12: Moving sub-arrays of 11 microphones with maximum search along the engine axis near the inlet, build 2 with lined inlet, shaft speed 78% N1

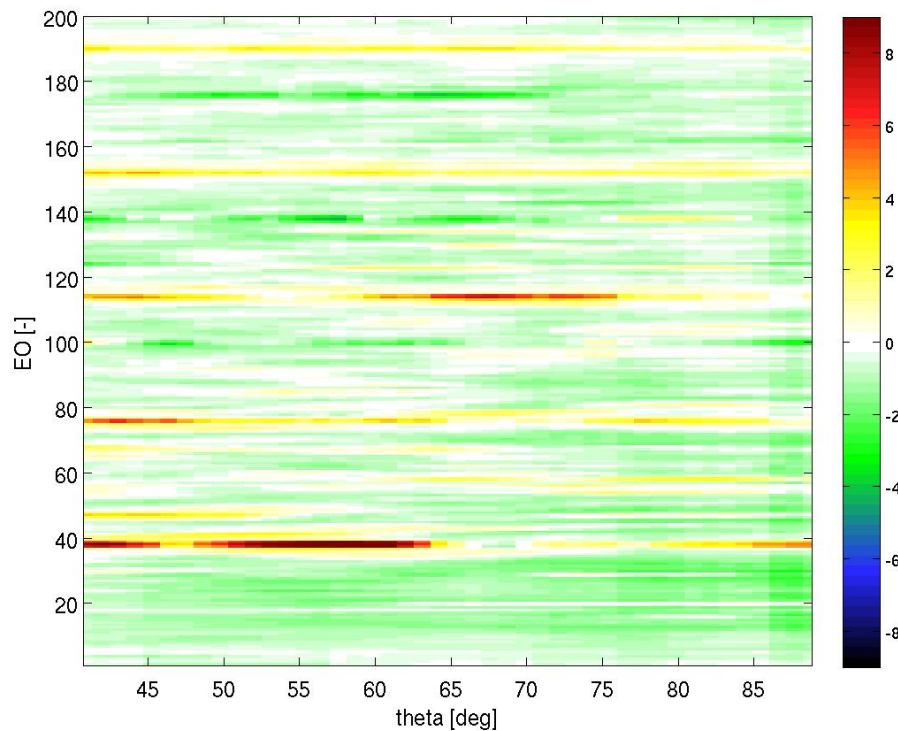


Figure 13: Moving sub-arrays of 11 microphones with maximum focused search, difference between build 2 (hard wall fan casing) and build 1 (lined fan casing), shaft speed 78% N1

### 3 ACKNOWLEDGEMENTS

This work has been performed in the framework of the project FREQUENZ with financial support from the German Federal Ministry of Economics and Technology (BMWi) under the Project FREQUENZ. The authors would like to thank Stefan Funke for his help during the experiments.

### REFERENCES

- [1] F. Arnold and H.A. Siller. Application of a phased microphone array to aero-engine combustion noise, 2003. AARC Core Noise Workshop, Phoenix, AZ, USA, February 26-27, 2003.
- [2] P. Böhning, H. Siller, K. Holland, F. Arnold, A. Kempton, and U. Michel. Novel methods for acoustic indoor measurements and applications in aero-engine test cells. DGLR Jahrbuch 2006/III, 2006. Deutscher Luft- und Raumfahrtkongress 2006, Braunschweig, November 9, 2006.
- [3] P. Böhning, H. Siller, K. Holland, F. Arnold, A. Kempton, and U. Michel. Novel methods for acoustic indoor measurements and applications in aero-engine test cells, 2006. Berlin Beamforming Conference (BeBeC) 2006, Berlin, November 21 and 22, 2006.
- [4] L. Enghardt, Y. Zhang, and W. Neise. Experimental verification of a radial mode analysis technique using wall-flush mounted sensors. 137th Meeting of the Acoustical Society of America, Berlin, March 15-19, 1999, 1999.
- [5] S. Guérin, U. Michel, H. Siller, U. Finke, and G. Saueressig. Airbus A319 database from dedicated flyover measurements to investigate noise abatement procedures. AIAA paper

- 2005-2981. 11th AIAA/CEAS Aeroacoustics Conference, Monterey, California, May 23-25, 2005.
- [6] S. Guidati, G. Guidati, and S. Wagner. A modification of the classical beamforming algorithm for reverberating environments, 2000. 7th International Congress on Sound and Vibration.
- [7] U. Michel, H.A. Siller, and Chr. Zwiener. Reduction of approach noise of the md11. AIAA paper 2006-2464, 2006. 12th AIAA/CEAS Aeroacoustics Conference, May 2006.
- [8] W. Neise and L. Enghardt. Technology approach to aero engine noise reduction. *Aerospace Science and Technology*, 7:352–363, 2003.
- [9] G. Saueressig, W. Dobrzynski, S. Guérin, S. Fröhlich, J. Jaeglè, M. Kiefner, M. Kutner, U. Michel, M. Pott-Pollenske, H.A. Siller, A. Uhl, and K. Haag. Investigation of noise reducing retrofit measures for existing aircraft, 2006. Euronoise 2006 conference, , May 30 - June 1, 2006.
- [10] P. Sijtsma and H. Holthusen. Corrections for mirror sources in phased array processing techniques, 2003. AIAA paper 2003-3196.
- [11] H.A. Siller, F. Arnold, and U. Michel. Investigation of aero-engine core-noise using a phased microphone array. AIAA paper 2001-2269, 2001. 7th AIAA/CEAS Aeroacoustics Conference, Maastricht, the Netherlands.
- [12] H.A. Siller and U. Michel. Buzz-saw noise spectra and directivity from flyover tests. AIAA paper 2002-2562, 2002. 8th AIAA/CEAS Aeroacoustics Conference, Breckenridge, Colorado, USA, June 17-19, 2002.
- [13] J. M. Tyler and T. G. Sofrin. Axial flow compressor noise studies. *Transactions of the Society of Automotive Engineers*, 70:309–332, 1962.